Origin of Deep Be Acceptor Levels in Nitride Semiconductors: The Roles of Chemical and Strain Effects

Xuefen Cai,[1] Jingxiu Yang,[1] Peng Zhang,[1,2,*] and Su-Huai Wei[1,†]

[1] *Beijing Computational Science Research Center, Beijing 100093, China*

[2] *College of Physics and Optoelectronic Engineering, Shenzhen University, Shenzhen, Guangdong 518060, China*

(Received 7 November 2018; revised manuscript received 1 January 2019; published 7 March 2019)

P type doping is often difficult in nitrides due to the high electronegativity of nitrogen. Beryllium (Be) is isovalent but more electronegative than Mg, so it is hoped that if Mg is replaced by Be as the dopant in nitride semiconductors, the acceptor level would be shallower. However, surprisingly, it is observed that the Be acceptor level is actually much deeper than that of Mg in nitride semiconductors. Based on the density functional theory (DFT) calculations with a hybrid functional, we systematically investigate the doping behaviors of Be and Mg acceptors in GaN and AlN. We reveal that the large local structural distortion around the Be dopant, as well as the large covalency of the Be—N bonds, are responsible for the deeper acceptor-transition-energy level of Be than that of Mg acceptors in GaN. Our results, therefore, provide a comprehensive understanding of chemical trends of *p* type doping in nitride semiconductors.

DOI: 10.1103/PhysRevApplied.11.034019

I. INTRODUCTION

The achievement of *p* type doping in nitride semiconductors, such as GaN and related alloys, has set the foundation for an entire semiconductor industry producing blue light-emitting diodes (LEDs) and lasers [1]. Mg is so far the only known effective *p* type dopant that can be realized in GaN. However, the doping efficiency in Mg-doped GaN is still limited, partially because of the relatively high-acceptor-transition-energy levels (approximately 250 meV), which has become the major bottleneck for the further development of nitride-based lighting devices. Therefore, searching for potentially shallow *p* type dopants in GaN or other nitride semiconductors, alternative to Mg, is of great importance and has attracted enormous attention for the past few decades.

Because Be 2*s* and 2*p* orbital energies are much deeper than the respective Mg 3*s* and 3*p* orbital energies (see Table I) and the acceptor wavefunction is more localized around the dopants, it is hoped that when Mg is replaced by Be, the acceptor level would be shallower in Be-doped system, that is, closer to the valence band maximum (VBM). Indeed, early theoretical calculations confirmed that Be doping in GaN exhibits a comparable solubility and an even shallower defect level than Mg [2,3]. Experimentally, a series of studies have also been carried out and some early studies have suggested that the ionization energy of Be acceptors in GaN(Be_{Ga}) could be less than 250 meV [4–8]. However, recent theoretical and experimental investigations [9–11] have challenged the early experimental results by suggesting that the Be_{Ga} acceptor level is actually much deeper (approximately 550 meV), and of note, so far, no practical lighting devices have been made based on Be-doped GaN. Also, the previous theoretical calculations that predicted Be_{Ga} as a shallow acceptor in GaN were based on density functional theory (DFT) with the local density approximation (LDA) functional, which is known to severely underestimate the band gaps of semiconductors and fail to accurately describe the localized hole states [2,3]. Actually, recent DFT calculations employing more sophisticated methods beyond the LDA have indicated that hole localization would occur for Be_{Ga} in GaN, which yields an acceptor level that is approximately 300 meV deeper than the corresponding Mg dopant (Mg_{Ga}) [9,10]. These calculations are supported by recent photo-induced electron paramagnetic resonance (EPR) measurements, which showed that the acceptor level of Be_{Ga} in GaN is approximately 700 meV above the VBM, that is, approximately 450 meV higher than that of Mg_{Ga} [11]. It seems that the expectation that Be doping can achieve efficient *p* type conductivity in GaN is not substantiated, but the physical origin behind the deep acceptor level of Be_{Ga} is still unclear. To further improve *p* type doping in GaN and related nitride alloys, which is important for a variety of potential applications, such as white light converters in monolithic white LEDs [12], it is important to understand the origin of this puzzling behavior.

In this work, based on first-principles calculations and detailed analysis, we show that the deep acceptor level

*pengzhang@szu.edu.cn
†suhuaiwei@csrc.ac.cn

 © 2019 American Physical Society

TABLE I. The valence s and p orbital energies ϵ (eV) for Be, Mg, Al, Ga, and N.

ϵ (eV)	Be	Mg	Al	Ga	N
s-orbital	−5.7	−4.9	−7.9	−9.2	−18.5
p-orbital	−2.2	−1.5	−2.9	−2.8	−7.3

of Be_{Ga} actually comes from a synergetic contribution of both the strain and chemical effects. Similar to previous calculations [10], we find significant asymmetric lattice distortions for both Be_{Ga} and Mg_{Ga} in their neutral charge states, while the distortions largely recover in their charged states when the valence p orbitals of the dopants are fully occupied, which leads to the deep transition energy levels, especially for Be_{Ga}. On the other hand, our calculations also indicate that the single-particle energy level of Be_{Ga} has a similar or even higher energy than that of Mg_{Ga} even without the lattice relaxation. This surprising result can be understood by noticing that due to the higher covalent Be—N bond, the reduced N $2p$ components of the defect states of Be_{Ga} below that of Mg_{Ga} will lead to a higher acceptor level. Our results, therefore, provide an alternative and comprehensive understanding of Be doping in GaN and other nitride semiconductors.

II. COMPUTATIONAL METHODS

Our calculations are carried out using the Heyd-Scuseria-Ernzerhof (HSE06) hybrid functional [13] and the projector augmented wave (PAW) method as implemented in VASP code [14,15]. A cut-off energy of 520 eV is used for the plane-wave basis set. For all the calculations, the atomic positions are relaxed until the Hellman-Feynman force on each atom is less than 0.01 eV/Å. For HSE06 calculations, we choose the Hartree-Fock exchange parameter $\alpha = 0.31$ for GaN to produce a band gap of 3.43 eV and $\alpha = 0.33$ for AlN to produce a band gap of 6.1 eV. Table II collects the calculated lattice parameters and band gaps of GaN and AlN in the wurtzite (WZ) structures together with the experimental data [16–18]. Our calculated lattice parameters for both GaN and AlN are in good agreement with experiments. In addition, the bond lengths of GaN and AlN, which consist of one axial bond (R_1) and three planar bonds (R_2), are also given in Table II. We find that for the WZ structure, the axial bond length is slightly larger than the planar bond length in both compounds.

For defect calculations, we construct a 96-atom supercell with a Γ-centered $2 \times 2 \times 2$ Monkhorst–Pack k mesh, where one Ga (or Al) atom is replaced by a single element dopant (Be or Mg). The spin-polarized calculations are carried out when there are unpaired electrons in the system. For the case of GaN, the formation energy $\Delta H_f(\alpha, q)$ for a defect α in the charge state q is calculated by [19]

$$\Delta H_f(\alpha, q) = \Delta E(\alpha, q) + n_{Ga}\mu_{Ga} + n_N\mu_N + n_D\mu_D + qE_F, \tag{1}$$

where $\Delta E(\alpha, q) = E(\alpha, q) - E(\mathrm{GaN}) + n_{Ga}E(\mathrm{Ga}) + n_N E(\mathrm{N}) + n_D E(D) + q\varepsilon_{VBM}(\mathrm{GaN})$. $E(\mathrm{GaN})$ is the total energy of the supercell and $E(\alpha, q)$ is the total energy of the same supercell but with a defect α. n_i is the number of elements and q is the number of electrons transferred from the supercell to the reservoirs in forming the defect cell. $\varepsilon_{VBM}(\mathrm{GaN})$ is the VBM energy of GaN and D (D is Mg or Be) is the single elemental dopant. μ_i is the chemical potential of atom i with respect to energy $E(i)$ for the bulk element i in the ground state.

Equation (1) show that the formation energy of a defect depends on the choice of chemical potentials. Consider, for instance, Be substitution on a Ga site, where the chemical potentials μ_{Ga} and μ_N vary over a range corresponding to the formation enthalpy of GaN[$\Delta H_f(\mathrm{GaN})$],

$$\mu_{Ga} + \mu_N = \Delta H_f(\mathrm{GaN}), \tag{2}$$

where the calculated $\Delta H_f(\mathrm{GaN})$ is −1.47 eV compared to the experimental value of −1.69 eV. [20]. Additionally, the chemical potentials are limited by the formation of elemental dopants and host elements,

$$\mu_{Ga} \le \mu(\mathrm{Ga}) = 0, \tag{3}$$

$$\mu_N \le \mu(\mathrm{N_2}) = 0, \tag{4}$$

$$\mu_{Be} \le \mu(\mathrm{Be}) = 0. \tag{5}$$

Finally, to avoid phase separation into Be_3N_2, we need to have

$$3\mu_{Be} + 2\mu_N \le \Delta H_f(\mathrm{Be_3N_2}). \tag{6}$$

Here, the calculated formation energy of Be_3N_2 is −6.77 eV ($\alpha = 0.31$), or −6.81 eV ($\alpha = 0.33$), compared to

TABLE II. Basic material properties for WZ GaN and AlN calculated using the HSE06 functionals: lattice parameters (*a, c/a, and u*), band gap (E_g), axial bond length (R_1), and planar bond length (R_2). Experimental values listed in the brackets for lattice parameters are from Ref. [18] and are from Refs. [16,17] for the band gaps.

	a (Å)	c/a	u	E_g (eV)	Bond length (Å)
GaN	3.19 (3.19)	1.63 (1.63)	0.38 (0.38)	3.43 (3.50)	$R_1 = 1.975$, $R_2 = 1.966$
AlN	3.11 (3.11)	1.60 (1.60)	0.38 (0.38)	6.10 (6.19)	$R_1 = 1.902$, $R_2 = 1.891$

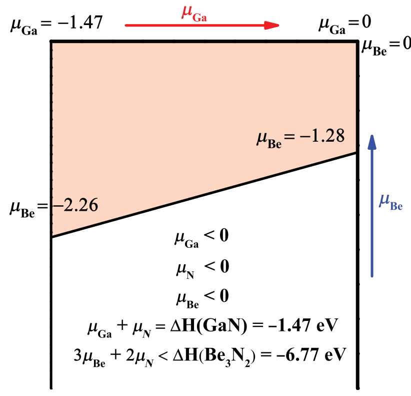

FIG. 1. Calculated chemical potential region for Be-doped GaN. The light pink shaded area is forbidden under the equilibrium growth condition.

the experimental value of −6.11 eV [10]. Using the equations above, we obtain the achievable chemical potential region, as shown in Fig. 1.

The transition energy level of a defect α between charge states q and q', $\varepsilon_\alpha(q/q')$, with respect to the VBM, is calculated from the formation energies by

$$\varepsilon_\alpha(q/q') = \frac{\Delta E(\alpha, q) - \Delta E(\alpha, q')}{q' - q} - \varepsilon_{\mathrm{VBM}}(\mathrm{GaN}). \quad (7)$$

Our convergence tests indicate that the 192-atom and 96-atom supercells yield very similar results. Therefore, we expect that the 96-atom cell is adequate to accurately describe the defect behaviors of Be and Mg in GaN.

III. RESULTS AND DISCUSSION

Figure 2 illustrates the calculated formation energies for Be and Mg acceptors in GaN and AlN, as functions of the Fermi level (FL). Both Ga-rich and Ga-poor (thus N-rich) conditions are considered. The range of the FL is from the VBM to a conduction band minimum (CBM), that is, from 0 to 3.43 eV for GaN and from 0 to 6.1 eV for AlN, respectively. In GaN, as shown in Figs. 2(a) and 2(b), the formation energies of Mg_{Ga} are lower than that of Be_{Ga} at both the Ga-rich and N-rich conditions, which should be ascribed to the smaller atomic size difference between Mg and Ga than that between Be and Ga. We find that both Be_{Ga} and Mg_{Ga} can form more easily under the N-rich condition than under the Ga-rich condition, which can be easily understood from Eq. (1). The (0/−1) transition level (which determines the ionization energy) of Mg_{Ga} is calculated to be approximately 0.26 eV above the VBM, in good agreement with previous calculations and experiments [10,21,22]. While for Be_{Ga}, a much deeper (0/−1) transition level of approximately 0.65 eV is found, which also falls in line with recent experimental results [10,11]. To address the optical properties of these defects, we show in Fig. 3 the calculated configuration coordinate diagrams for the optical processes of Mg and Be in GaN. The optical transition levels correspond to the absorption and emission energies between the defect levels and the CBM. From our calculations, we estimate an optical emission peak at 2.59 eV for Mg_{Ga}, which is consistent with the theoretical values and experimental observed peak in GaN (approximately 2.7–2.9 eV) [21,22]. The predicted optical transition level of 1.67 eV for Be_{Ga} is apparently smaller than the observed PL lines in some early papers [22], but in agreement with recent theoretical and experimental results (approximately 1.8–2.2 eV) [10,11]. Apparently, more accurate experimental measurements and theoretical predictions are needed. Furthermore, to validate our results, we also perform the constrained DFT calculation [23]. Although the calculated acceptor levels using constrained DFT for Mg_{Ga} (approximately 0.20 eV) and Be_{Ga} (approximately 0.60 eV) are slightly smaller compared with the conventional method because they contain the exciton binding energy, we find the transition energy level of Be_{Ga} is still much deeper than that of Mg_{Ga} in GaN.

For comparison, we also calculate the Be and Mg doping in AlN, as shown in Figs. 2(c) and 2(d). As in GaN, we find that the formation energies of Mg_{Al} are smaller than that of Be_{Al} under both the Al-rich and N-rich conditions and the formation of Mg_{Al} and Be_{Al} both favor the N-rich condition. The (0/−1) transition levels for Mg_{Al} and Be_{Al} in AlN are calculated to be 0.71 and 1.10 eV, respectively, both of which are much deeper than those in GaN. This is due to the fact that AlN has a lower VBM energy (approximately 0.80 eV) than GaN because of the absence of the occupied semicore 3d orbitals and thus the lack of p−d repulsion in AlN, which acts to raise the VBM energy in GaN [24]. These results clearly indicate that the Be doping would generally yield much deeper acceptor levels in nitride semiconductors than Mg doping, and therefore, cannot produce efficient p type conductivity, which is in accordance with the fact that no practical lighting devices based on Be-doped nitrides have ever been produced. However, on the other hand, these results apparently contradict the conventional understanding that a more electronegative dopant (Be vs Mg) should introduce a shallower acceptor level rather than a deeper one [25].

In the previous work, Lyons *et al.* [10] speculated that the deeper acceptor level of Be_{Ga} than Mg_{Ga} is due to the smaller atomic size of Be than Mg, which results in a larger lattice distortion around the Be_{Ga} in its neutral state Be^0_{Ga}, and also a greater hole localization. Indeed, the local lattice distortion and hole localization for both Be^0_{Ga} and Mg^0_{Ga} in GaN are also found in our calculations, as shown in Figs. 4(a) and 4(c). We find that due to the large size difference between Be and Ga, the local lattice distortion of Be^0_{Ga} is much larger than that of Mg^0_{Ga}. In the Be^0_{Ga} case, the Be atom is displaced along the $[000\bar{1}]$ direction,

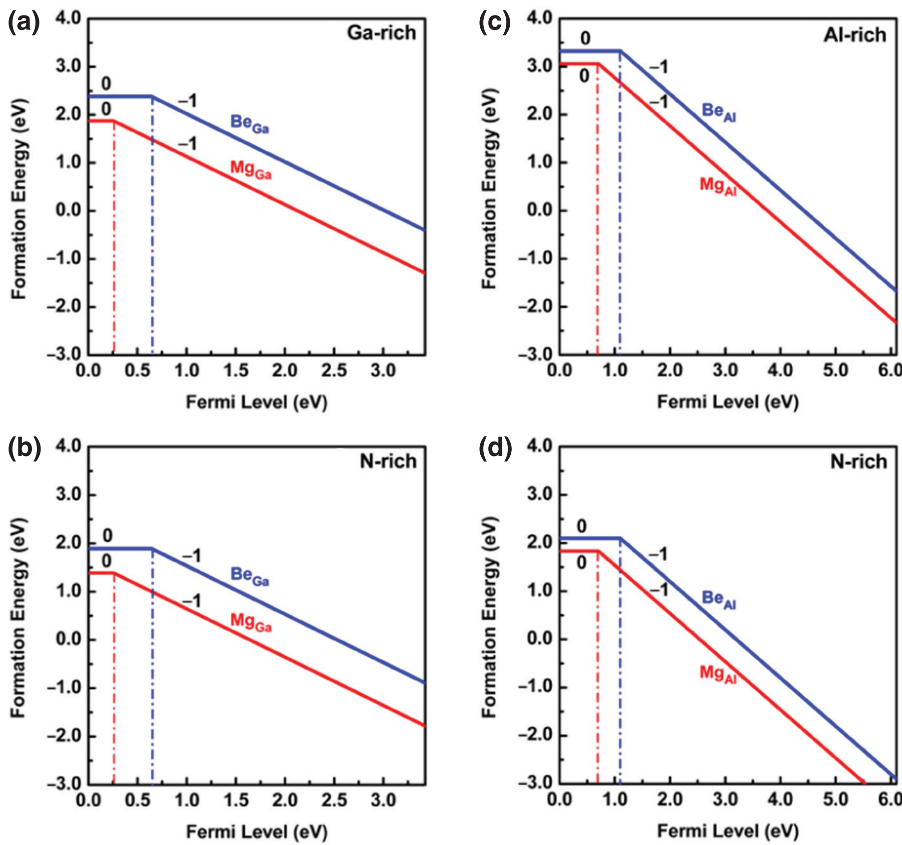

FIG. 2. Calculated formation energies for Be_{Ga} and Mg_{Ga} in GaN under (a) Ga-rich and (b) N-rich conditions, as well as that for Be_{Al} and Mg_{Al} in AlN under (c) Al-rich and (d) N-rich conditions, as a function of FL. Note the different energy scales in the GaN and AlN systems. The slope of the formation energy segment gives the charge state of the corresponding defect and the Fermi energy at which the slope changes indicates the (0/–) transition energy level. The zero of the FL is at the VBM.

forming a much shorter in-plane Be—N bond, whereas the Be—N bond along the axial direction is increased by 38% compared to the bulk *Ga—N* bond length, that is, it is essentially broken [Fig. 4(a)]. For Mg_{Ga}^{0}, a similar displacement is observed, but to a lesser degree [Fig. 4(c)]. The Mg—N bond along the axial direction is increased by 17%. This displacement is the main reason that the defect charge is localized on a single N next to the impurity. For the full-shell negatively charged states Be_{Ga}^{-1} and Mg_{Ga}^{-1}, the local trigonal lattice distortions are largely recovered and the hole localization disappears, as shown in Figs. 4(b) and 4(d). In this case, only breathing relaxation of the lattice is observed, with the nearest-neighbor N atoms all moving away from the dopant by 5% for Mg_{Ga}^{-1} and moving close to the dopant by 6% for Be_{Ga}^{-1}, respectively. As a result, large relaxation-energy differences between the neutral and negatively charged states are obtained (1.6 eV for Be_{Ga}^{-1} and 0.95 eV for Mg_{Ga}^{-1}), which indicate that the strain effect plays an important role in determining the defect levels of Be and Mg acceptors in GaN.

Beside the lattice distortion, however, other possible factors that could influence the defect levels of Be and Mg acceptors in GaN have rarely been discussed, although

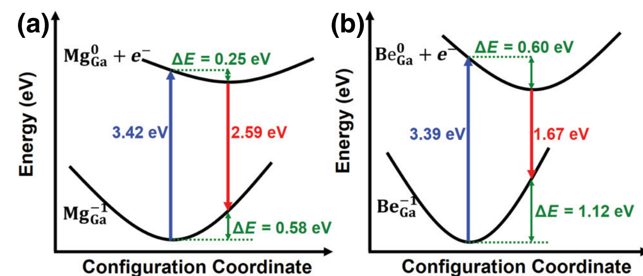

FIG. 3. Configuration coordinate diagrams for the optical processes of (a) Mg and (b) Be in GaN.

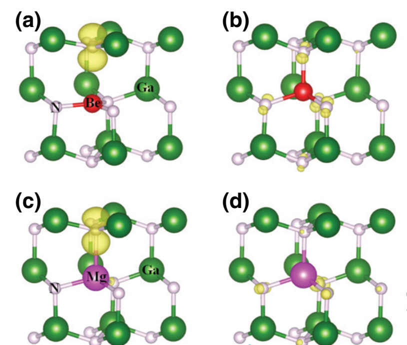

FIG. 4. The local relaxed geometry and three-dimensional (3D) partial charge density (yellow: isosurface of0.01 e^{-}/Bohr^{3}) for neutral defect states of (a) Be_{Ga}^{0}, (c) Mg_{Ga}^{0}, and negatively charged states of (b) Be_{Ga}^{-1} and (d) Mg_{Ga}^{-1} in GaN. The green-colored circle is for Ga, the gray one is for N, the red one is for Be, and the purple one is for Mg.

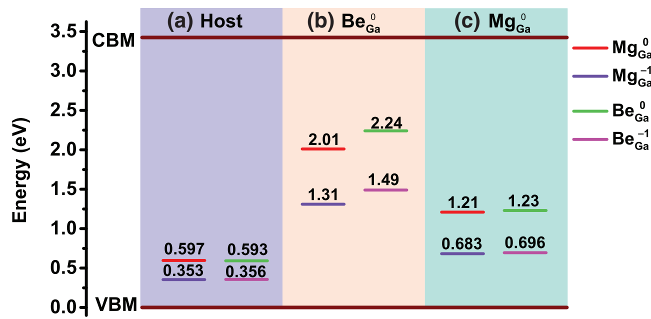

FIG. 5. The single-particle levels of Mg^0_{Ga}, Mg^{-1}_{Ga}, Be^0_{Ga}, and Be^{-1}_{Ga} calculated under the fixed (a) host structure, (b) fully-relaxed structure of Be^0_{Ga}, and (c) Mg^0_{Ga}.

these factors may also be significant. Figure 5 plots the calculated single-particle-energy levels for the neutral and negatively charged states for both Be and Mg acceptors in GaN. To eliminate the influence of the strain, we fix the structural parameters to the values of the host structure, the fully relaxed structures of Be^0_{Ga} and Mg^0_{Ga}, respectively, and perform no further structural relaxation when the defects are either in neutral or charged states. As shown in Fig. 5(a), for both neutral and negatively charged states in the host structure, we find that the single-particle level of the Be acceptor has almost the same energy as that of the Mg acceptor with an energy difference of the order of only a few meV. This is because in the host structure, the defect wavefunction is less localized, thus the energy level does not depend very much on the dopants. However, in the fixed Be^0_{Ga} and Mg^0_{Ga} structures, the single-particle levels of both Be^0_{Ga} and Be^{-1}_{Ga} are shown to be deeper than the corresponding Mg counterparts, especially for the fixed Be^0_{Ga} structure, as shown in Figs. 5(b) and 5(c). Given the fact that Be is more electronegative than Mg, these results are quite surprising and cannot be simply explained by the stain effect, which is already turned off.

To clarify this ambiguity, we carefully investigate the bonding properties between the dopants and the nearest-neighbor N atoms. Figure 6(a) plots the deformation charge density for the chemical bonds between the dopant and the N atoms within the basal plane for both Be^0_{Ga} and Mg^0_{Ga} in the host structure. The deformation charge density is defined as the difference between the total charge density in a solid and the superposition of independent atomic charge densities placed at the atomic sites of the same solid, and thus indicates the charge transfer when the chemical bonds are formed. From Fig. 6(a), it is obvious that a significant amount of charge transfer from the Mg to N atoms occurs when the Mg—N bonds are formed, reflecting the major ionic character of the bonds. While for Be—N bonds, on the other hand, a large amount of charge is found between the Be and N atoms, forming more directional and covalent bonds. Since the single-particle levels shown in Fig. 5(a) are dominated by the N $2p$ orbitals hybridized with some dopant (D) p orbitals, more covalent D—N bonds mean larger contributions of D p orbitals on these levels. Because the dopant p level has higher energy than the N p level, this in turn raises their energy [26]. These can be understood by noticing that ε^p_N is closer to

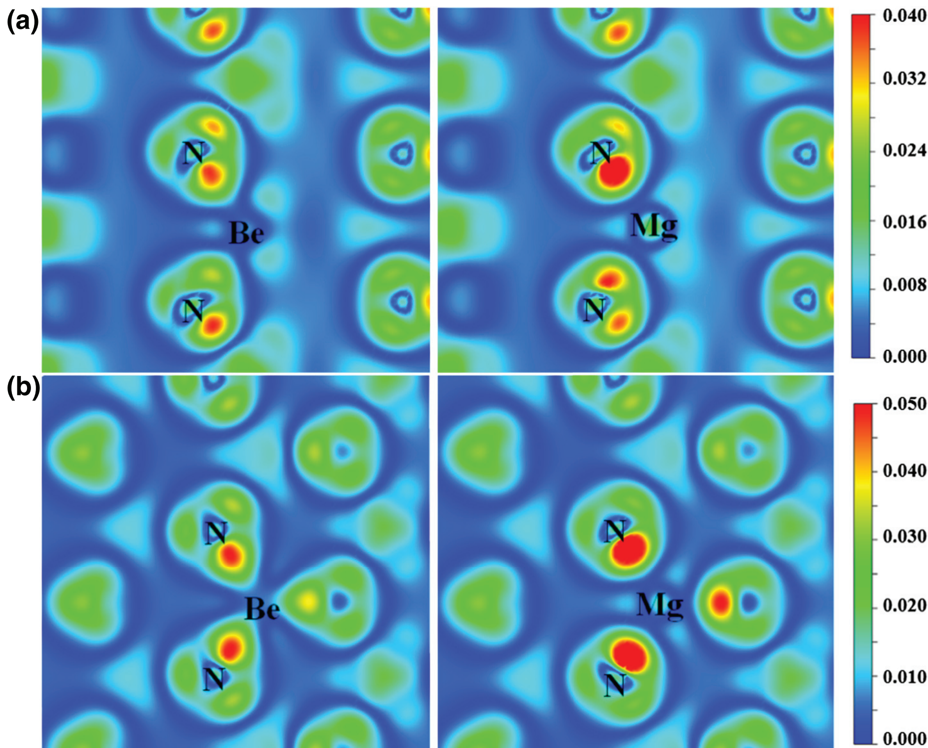

FIG. 6. The deformation charge density in the plane of D—N bonds for both Be^0_{Ga} and Mg^0_{Ga} in the (a) host and (b) Be^0_{Ga} structure, in units of e/Bohr^3.

$\varepsilon^p_{\mathrm{Be}}$ than to $\varepsilon^p_{\mathrm{Mg}}$ (see Table I), so the Be—N bonds are more covalent than Mg—N bonds. Thus, there is a larger hybridization between Be 2p and N 2p orbitals, leading to a higher contribution of the Be 2p orbitals to the defect energy level than that of the Mg 3p orbitals. As a result, in the host structure, although Be is more electronegative than Mg, the effect is largely cancelled by the larger component of Be 2p orbitals in the $\mathrm{Be_{Ga}}$ defect level, which pushes its energy up. These results indicate that the chemical effect or the covalency of D—N bonds also plays a significant role in determining the doping behavior of Be and Mg acceptors in GaN.

Figure 6(b) plots the deformation charge density of D—N bonds for both $\mathrm{Be^0_{Ga}}$ and $\mathrm{Mg^0_{Ga}}$ in the $\mathrm{Be^0_{Ga}}$ structure. It is clear to see that the structural distortion profoundly changes D—N bonds. As shown in Fig. 4, when the doping atom moves toward the center of the three N atoms within the basal plane after the distortion, the D—N bond length (R_2) decreases from 1.966 to 1.730 Å, which enhances the hybridization between D and N p orbitals. We find that the enhancement of the covalency of Be—N bonds is greater than that of Mg—N bonds, as illustrated in Fig. 6(b). As a consequence, the chemical effect pushes the single-particle levels of Be acceptors further above that of Mg acceptors, as shown in Fig. 5(b). These results imply an apparent response of the chemical effect to the strain effect, both of which then synergistically result in a deeper acceptor level of $\mathrm{Be_{Ga}}$ than that of $\mathrm{Mg_{Ga}}$ in GaN and other nitride semiconductors. Although not explicitly given here, a similar conclusion can also explain the results in other nitride semiconductors, such as AlN and (Ga,Al)N alloys.

IV. CONCLUSION

In summary, we perform first-principles hybrid functional calculations to systematically study the doping properties of both Be and Mg acceptors in GaN. Our results show that the transition-energy levels of the Be acceptor lie much deeper than those of Mg in GaN, which is consistent with the recent experimental observations [11]. We find that this unusual deep defect level of the Be acceptor originates from a synergetic combination of both the strain and chemical effects. Moreover, the chemical effect is found to be closely related to the covalency of the bonds between the dopant atoms and host anions, which also has a spontaneous response to the local structural distortion and thus the strain effect. Our results, therefore, significantly broaden the understanding of Be doping in nitride semiconductors and provide a guideline for the further control of the defect properties in nitride-based electronic and optical devices.

ACKNOWLEDGMENTS

This work is supported by the Science Challenge Project, under Grants No. TZ2016003 and No. TZ2018004, the National Key Research and Development Program of China (Grant No. 2016YFB0700700), and Nature Science Foundation of China (Grants No. 51672023, No. 11634003, and No. U1530401). We also acknowledge the computational support from the Beijing Computational Science Research Center (CSRC).

[1] S. Pimputkar, J. S. Speck, S. P. DenBaars, and S. Nakamura, Prospects for LED lighting, Nat. Photonics **3**, 180 (2009).

[2] J. Neugebauer and C. G. Van de Walle, Chemical trends for acceptor impurities in GaN, J. Appl. Phys. **85**, 3003 (1999).

[3] C. G. Van de Walle, S. Limpijumnong, and J. Neugebauer, First-principles studies of beryllium doping of GaN, Phys. Rev. B **63**, 245205 (2001).

[4] D. Dewsnip, A. Andrianov, I. Harrison, J. Orton, D. Lacklison, G. Ren, S. Hooper, T. Cheng, and C. Foxon, Photoluminescence of MBE grown wurtzite Be-doped GaN, Semicond. Sci. Technol. **13**, 500 (1998).

[5] F. Sánchez, F. Calle, M. Sanchez-Garcia, E. Calleja, E. Munoz, C. Molloy, D. Somerford, J. Serrano, and J. Blanco, Experimental evidence for a Be shallow acceptor in GaN grown on Si (111) by molecular beam epitaxy, Semicond. Sci. Technol. **13**, 1130 (1998).

[6] C. Ronning, E. Carlson, D. Thomson, and R. Davis, Optical activation of Be implanted into GaN, Appl. Phys. Lett. **73**, 1622 (1998).

[7] S. Sugita, Y. Watari, G. Yoshizawa, J. Sodesawa, H. Yamamizu, K.-T. Liu, Y.-K. Su, and Y. Horikoshi, Growth of Be-doped p-type GaN under invariant polarity conditions, Jpn. J. Appl. Phys. **42**, 7194 (2003).

[8] A. Salvador, W. Kim, Ö Aktas, A. Botchkarev, Z. Fan, and H. Morkoç, Near ultraviolet luminescence of Be doped GaN grown by reactive molecular beam epitaxy using ammonia, Appl. Phys. Lett. **69**, 2692 (1996).

[9] S. Lany and A. Zunger, Dual nature of acceptors in GaN and ZnO: The curious case of the shallow MgGa deep state, Appl. Phys. Lett. **96**, 142114 (2010).

[10] J. L. Lyons, A. Janotti, and C. G. V. d. Walle, Impact of group-II acceptors on the electrical and optical properties of GaN, Jpn. J. Appl. Phys. **52**, 08JJ04 (2013).

[11] W. R. Willoughby, M. E. Zvanut, J. Dashdorj, and M. Bockowski, A model for Be-related photo-absorption in compensated GaN:Be substrates, J. Appl. Phys. **120**, 115701 (2016).

[12] H. Teisseyre, M. Bockowski, I. Grzegory, A. Kozanecki, B. Damilano, Y. Zhydachevskii, M. Kunzer, K. Holc, and U. T. Schwarz, GaN doped with beryllium—An effective light converter for white light emitting diodes, Appl. Phys. Lett. **103**, 011107 (2013).

[13] J. Heyd, G. E. Scuseria, and M. Ernzerhof, Hybrid functionals based on a screened Coulomb potential, J. Chem. Phys. **118**, 8207 (2003).

[14] G. Kresse and J. Furthmüller, Efficiency of ab-initio total energy calculations for metals and semiconductors using a plane-wave basis set, Comput. Mater. Sci. **6**, 15 (1996).

[15] G. Kresse and J. Furthmüller, Efficient iterative schemes for ab initio total-energy calculations using a plane-wave basis set, Phys. Rev. B **54**, 11169 (1996).

[16] B. Monemar, Fundamental energy gap of GaN from photoluminescence excitation spectra, Phys. Rev. B **10**, 676 (1974).

[17] D. Brunner, H. Angerer, E. Bustarret, F. Freudenberg, R. Höpler, R. Dimitrov, O. Ambacher, and M. Stutzmann, Optical constants of epitaxial AlGaN films and their temperature dependence, J. Appl. Phys. **82**, 5090 (1997).

[18] H. Morkoç, *Handbook of Nitride Semiconductors and Devices* (Weily, New York, 2008), Vol. 1-3.

[19] S.-H. Wei and S. B. Zhang, Chemical trends of defect formation and doping limit in II-VI semiconductors: The case of CdTe, Phys. Rev. B **66**, 155211 (2002).

[20] M. Ranade, F. Tessier, A. Navrotsky, V. Leppert, S. Risbud, F. DiSalvo, and C. Balkas, Enthalpy of formation of gallium nitride, J. Phys. Chem. B **104**, 4060 (2000).

[21] J. L. Lyons, A. Janotti, and C. G. Van de Walle, Shallow Versus Deep Nature of Mg Acceptors in Nitride Semiconductors, Phys. Rev. Lett. **108**, 156403 (2012).

[22] M. A. Reshchikov and H. Morkoç, Luminescence properties of defects in GaN, J. Appl. Phys. **97**, 5 (2005).

[23] Y. Zhang and J. Wang, Bound exciton model for an acceptor in a semiconductor, Phys. Rev. B **90**, 155201 (2014).

[24] S.-H. Wei and A. Zunger, Valence band splittings and band offsets of AlN, GaN, and InN, Appl. Phys. Lett. **69**, 2719 (1996).

[25] Y. Yan and S.-H. Wei, Doping asymmetry in wide-bandgap semiconductors: Origins and solutions, Phys. Stat. Sol. (b) **245**, 641 (2008).

[26] W. Harrison and J. Tersoff, Tight-binding theory of heterojunction band lineups and interface dipoles, J. Vac. Sci. Technol., B: Microelectron. Process. Phenom. **4**, 1068 (1986).